Critical behavior of a three-dimensional random-bond Ising model using finite-time scaling with extensive Monte Carlo renormalization-group method

Wanjie Xiong,[1,2] Fan Zhong,[1,*] Weilun Yuan,[1] and Shuangli Fan[1]

[1]*State Key Laboratory of Optoelectronic Materials and Technologies, School of Physics and Engineering, Sun Yat-sen University, Guangzhou 510275, People's Republic of China*

[2]*Department of Applied Physics, College of Science, South China Agricultural University, Guangzhou 510640, People's Republic of China*

(Received 22 February 2010; published 25 May 2010)

We have investigated the critical behavior of a three-dimensional random-bond Ising model for a series of the disorder strength by a finite-time scaling combining with Monte Carlo renormalization-group method in the presence of a linearly varying temperature. The method enables us to estimate a lot of critical exponents of both static and dynamic nature independently as well as the critical temperatures. The static exponents obtained agree well with most existing results, verify both the hyperscaling and the Rushbrooke scaling laws and their combined scaling law, which in turn validate their asymptotic nature, and corroborate the universality of the relevant random fixed point with respect to the forms of disorder. The dynamic critical exponent z is estimated to 2.114(51), which is compatible with those obtained from experiments and renormalization-group analyses. The exponents at low and high disorder strengths do not satisfy all scaling laws and are argued to be crossover exponents that reflect crossover from the random fixed point to the pure and the percolation fixed point. They also indicate that the exponents that were previously suggested to be a distinct universality class for strong disorder strength in the literature may be just crossover. Our results demonstrate the effectiveness of the finite-time scaling method.

DOI: 10.1103/PhysRevE.81.051132 PACS number(s): 64.60.Ht, 75.10.Nr, 05.10.Ln, 75.40.−s

I. INTRODUCTION

Any real materials will inevitably contain impurities, whose effects on phase transitions are thus of great importance. For a pure system exhibiting a second-order or continuous phase transition, the effects of disorder are well known from the Harris criterion [1,2], namely, uncorrelated quenched randomness coupled to local energy density is irrelevant and the universality class of the pure system persists when its specific-heat critical exponent $\alpha<0$, while such randomness will lead to a new universality class controlled by a new random fixed point when $\alpha>0$. The Ising model is a paradigmatic model to test the prediction. In two-dimensional (2D), its $\alpha=0$, which is the marginal case and has attracted great interest in the past years [3]. In three-dimensional (3D), its $\alpha=0.1103(1)>0$ [4]. Accordingly, disorder is relevant and a random fixed point characterized by new critical exponents is expected. Recent experiments have showed that the critical exponents of the site-diluted Ising model are different from the corresponding pure version and are independent on impurity concentrations for sufficiently low ones [5,6]. The field-theoretic studies on the 3D Ising model in the present of weakly diluted quenched disorder have reached a level of up to six loops in the renormalization-group (RG) analysis and have also confirmed the random fixed point [5,7]. Also, high-temperature series expansions of the susceptibility provided evidence for the random fixed point by existence of a plateau in the variation in the critical exponent γ with bond-diluted concentrations [8]. Numerical investigations of the 3D disordered Ising model have also found different critical exponents. However, usual methods always obtain apparent exponents that depend on the strength of disorder in contradiction to the expectation of a single random fixed point [5]. These exponents may be only effective that contain effects from corrections to scaling and/or may reflect crossover arising from the competition of the random fixed point with the pure and also the percolation fixed point. These complexity and also possible lack of self-averaging [9] make it difficult to correctly identify the asymptotic critical exponents at the random fixed point. Dilution-independent numerical results were first achieved by taking into account corrections to scaling and a subsequent proper infinite volume extrapolation in a 3D site-diluted Ising model [10], a later study found it difficult, however, to extract the correction-to-scaling exponent in a bond-diluted Ising model [11]. To avoid the difficulties, temperature scalings of the susceptibility and magnetization were invoked to obtain concentration-independent critical exponents [11]. Another solution is to select a particular spin concentration [10,12–14] which was estimated to suppress corrections to scaling or crossover effects [15–17].

So far, the static critical exponents obtained from RG analysis, [7] Monte Carlo (MC) simulations [10,11,16,18,19], and experiments [6] agree in general quite well. However, $\gamma=1.306$ from a nonperturbative approach [20] and $\gamma=1.305(5)$ from a high-temperature series expansion [8] are slightly smaller than $\gamma=1.400(30)$ [6], $\gamma=1.330(17)$ [7], $\gamma=1.342(10)$ [10], $\gamma=1.341(4)$ [16], $\gamma=1.342(7)$ [18], and also $\gamma=1.34(1)$ of the bond-diluted Ising model [11]. Also, there is a small difference between the experimental $\alpha=-0.10(2)$ [6] and other results of $\alpha=-0.034(30)$ [7], $\alpha=-0.051(9)$ [10], and $\alpha=-0.049(6)$ [16]. So is the leading correction-to-scaling exponent [14]. Be-

*Corresponding author; stszf@mail.sysu.edu.cn

sides, a recent investigation suggested that there are two universality classes corresponding to strong and weak dilutions [18,21]. Thus, further investigations are still needed.

In addition, there exists an issue concerning with the validity of the scaling laws [2]. Up to now, most investigations including the RG analyses [7,22] produced results of ν, η, and/or γ. Other exponents were derived from the scaling laws. However, in some cases, the random-field Ising model for instance, at least one of them is indeed broken [23]. Although in the present case, no evidence indicates that they would be broken, their direct numerical verifications are rare. On the other hand, owing to the difficulty in determining asymptotic critical exponents as mentioned above and the fact that the perturbative series of RG functions are not Borel summable [24], whether or not the obtained exponents are asymptotic is a serious question. A method to check is thus to test them with the scaling laws if they are valid because asymptotic critical exponents should then satisfy them although the reverse is not necessarily true. In fact, validity of the scaling laws, $\gamma=\nu(2-\eta)$ in the six-loop RG analysis [7], for instances, has been invoked to reckon the correctness of the obtained exponents. On the other hand, in the bond-diluted Ising model, the scaling law $2\beta/\nu+\gamma/\nu=d$ (d the space dimensions) was found to be satisfied by effective exponents of several different dilutions [11]. Therefore, it is desirable to test the scaling laws to check both the validity of the laws themselves and the problem of the asymptotic nature of the exponents obtained.

Dynamics of the disordered Ising model has also been extensively studied. However, the dynamical critical exponent z obtained shows less agreement. Early perturbative RG results yielded $z\approx 2.336$ [25] and $z\approx 2.11$ [26]. Subsequent RG analysis with resummation techniques of two- to three-loop dynamical functions gave $z=2.237$ [27], $z=2.180$ [28], $z=2.191$ [29], $z=2.165$ [30], $z=2.172$ [31], and $z=2.1792(4)$ [32], all of which appear to agree with $z=2.18(10)$ of experimental measurements on both $Fe_{0.9}Zn_{0.1}F_2$ [33] and $Fe_{0.93}Zn_{0.07}F_2$ [34]. Numerical simulations again produced results that were disorder dependent [35–39]. Then, within a small disorder range, $z(p=0.95)=2.19(7)$ and $z(p=0.8)=2.20(8)$ varied little and were suggested to be asymptotic [35], a value which appeared to agree with the RG results, where p is the spin concentration. On the other hand, suppressing effects of crossover [36] or corrections to scaling [37,38] with a particular spin concentration yielded $z=2.4(1)$ for $p\approx 0.8$ [36], $z=2.62(7)$ for $p=0.63$ [37], $z=2.6(1)$ for $p=0.8$ [38], and $z=2.35(2)$ for $p=0.8$ [39]. Whereas the middle two [37,38] of nonequilibrium results were quite close though the concentration that suppressed corrections differed and the correction-to-scaling exponent was not quite consistent and was not compatible with the static one [10] as predicted by field theories [28], the latter [39] confirmed this and the universality against equilibrium and nonequilibrium results. It also agrees with $z=2.36(9)$ found in the high-temperature paramagnetic phase [14]. However, a recent investigation by short-time critical dynamic method obtained close results between $p=0.95$ and $p=0.8$ with an average $z=2.196(17)$ after taking corrections to scaling into account [19], in agreement with another previous MC result of $z=2.2(1)$ for $p=0.85$ again in an attempt to minimize corrections to scaling [13]. Note that we have only considered local dynamics arising from the single-spin Metropolis algorithm [40] that is believed to fall in the identical universality class with those observed experimentally and studied analytically by field theory. Cluster algorithms such as the Swendsen-Wang [41] and the Wolff algorithm [42] exhibit entirely distinct dynamic behavior [11,13,43] due to their nonlocality and will not be considered hereafter.

Yet another issue that is less studied is the question of universality of a random fixed point with respect to the forms of disorder [11,16,17,39]. The site-diluted, the bond-diluted, and the $\pm J$ Ising model are the three usual studied disordered Ising models. They have been suggested to belong to a single universality class as their fixed-point Hamiltonian was found to be coincident in a numerical RG study [17]. The first two models have also been estimated to share the same static critical exponents by MC simulations [11,16]. Also the dynamical critical exponent z of the three models has been found to be identical [39]. An extension of the bond-diluted model is a random-bond Ising model (RBIM) in which the coupling J can select randomly from two values. If one of the two values is zero, it reduces to the former model. In 2D, the RBIM has been studied and suggested to show weak universality in which exponent ratios such as γ/ν keep constant though individual exponents vary with disorder strengths [44]. Here, we shall study the model to investigate the universality.

In order to study these issues, we shall apply in this paper a finite-time scaling [45] combining with an extensive Monte Carlo renormalization group (MCRG) approach in the presence of a linearly varying temperature [46,47] to study the critical behavior of the 3D RBIM. The linearly varying temperature drives the system out of equilibrium in such a way that there is a finite-time scale proportional to the inverse of the temperature sweep rate that can probe effectively the slow dynamics induced by the randomness although the usual Metropolis algorithm [40] is utilized. The critical exponents ν, z, β, α, and γ for various disorder amplitudes so estimated independently and confirmed by scaling plots of data collapses enable us to check the validity of the hyperscaling law, the Rushbrooke scaling law, and their combined scaling law. These enable us in turn to identify the asymptotic critical behavior controlled by the relevant random fixed point and also possible crossover effects from the fixed point to the tricritical and also to the possible percolation fixed point. The static exponents obtained agree well with most existing results, verify the three scaling laws, which in turn validate their asymptotic nature, and corroborate the universality of the random fixed point. The dynamic critical exponent is estimated to 2.114(51), which is compatible within the statistical errors with those obtained from experiments and RG analysis but not supports recent results of bigger values. Crossover exponents are also indicated at low and high disorder strengths that do not satisfy all scaling laws. The exponents at the high disorder strength appear close to those that were suggested to belong to a new class, indicating that the latter may probably just be crossover too.

The structure of the rest is the following. Section II presents the model and the method used, and Sec. III estimates the critical temperature and the critical exponents for various

disorder amplitudes. Analysis and discussions of the results are given in Sec. IV, with conclusions summarized in Sec. V.

II. MODEL AND METHOD

A. Model

The Hamiltonian of the RBIM is

$$H = -\sum_{\langle i,j\rangle} J_{ij} S_i S_j, \tag{1}$$

where the classical spin $S_i = \pm 1$ and $\langle i,j\rangle$ denotes the sum over nearest-neighbor spin pairs on a cubic lattice. The interaction strength J_{ij} can select from two positive values, J_1 and J_2, with probability p and $1-p$. The disorder amplitude is defined as $r_0 = J_2/J_1$. The pure system corresponds to $r_0 = 1$ and the usual bond-diluted model to $r_0 = 0$. Here we only consider the case in which $p = 0.5$. The physical observables considered are the order parameter, the specific heat per site, the magnetic susceptibility, and the nearest-neighbor correlation function, which are defined, respectively, as

$$M = \frac{1}{N}\sum_i S_i, \tag{2}$$

$$C = \frac{L^d}{T^2}(\langle E^2\rangle - \langle E\rangle^2), \tag{3}$$

$$\chi = \frac{L^d}{T}(\langle M^2\rangle - \langle M\rangle^2), \tag{4}$$

$$G_{nn} = \left\langle \frac{1}{dN}\sum_{\langle i,j\rangle} S_i S_j \right\rangle - \langle M\rangle^2, \tag{5}$$

where N is the total number of spins, L is the lattice size used, T is the temperature, E is the energy per site, and the angle brackets denote averages.

B. Finite-time scaling

Finite-size scaling is an effective method to extract critical exponents [2]. The idea of finite-time scaling has been used in simulated annealing [48] and forced oscillation [49]. Recently, it is realized that the inverse rate of the sweeping external field represents a controllable effective finite-time scale that is the temporal analog of the length scale in finite-size scaling and that affects the scaling of the system. A RG theory of finite-time scaling is thus systematically proposed [45]. Here, we shall apply the finite-time scaling in the case of a linearly varying temperature to estimate critical exponents.

According to the theory of finite-time scaling [45], the order parameter, for instance, transforms under a length rescaling of factor b as

$$M(T,R) = b^{-\beta/\nu} M(\tau b^{1/\nu}, R b^r) \tag{6}$$

or the reduced temperature $\tau = T - T_c$, the sweep rate of the temperature R, and the time t transform as

$$R' = R b^r,$$

$$\tau' = \tau b^{1/\nu},$$

$$(t - t_c)' = (t - t_c) b^{-z}, \tag{7}$$

where T_c is the critical temperature, r is a rate exponent, and t_c is the time at which $T = T_c$. For the linear sweep, $\tau = R(t - t_c)$, one finds a scaling law from Eq. (7) [45,50,51]

$$r = z + 1/\nu, \tag{8}$$

which may be regarded as a definition of r.

Finite-time scaling forms of the order parameter can therefore be found from Eq. (6),

$$M(T,R) = R^{\beta/r\nu} f_1(\tau R^{-1/r\nu}). \tag{9}$$

Similarly, the nonequilibrium susceptibility and the specific heat obey, respectively,

$$\chi(T,R) = R^{-\gamma/r\nu} f_2(\tau R^{-1/r\nu}), \tag{10}$$

$$C(T,R) = C_0 + R^{-\alpha/r\nu} f_3(\tau R^{-1/r\nu}) \quad \text{for} \quad \alpha < 0, \tag{11}$$

$$C(T,R) = R^{-\alpha/r\nu} f_4(\tau R^{-1/r\nu}) \quad \text{for} \quad \alpha > 0, \tag{12}$$

where all fs are scaling functions and C_0 is a constant. Equation (12) describes the case in which the specific heat diverges at criticality and thus possessing a positive α, while Eq. (11) describes the case in which the specific heat exhibits a finite cusp at the critical point and thus possessing a negative α. These scaling forms themselves allow us to find the critical exponents by optimal data collapsing and thus check the validity of scaling similar to the method of finite-size scaling.

Nevertheless, to facilitate the estimate of the exponents, one notes that at $T = T_c$ at which $\tau = 0$, all fs are regular. As a consequence, one obtains from Eqs. (10)–(12)

$$M(T_c,R) \sim R^{\beta/r\nu}, \tag{13}$$

$$\chi(T_c,R) \sim R^{-\gamma/r\nu}, \tag{14}$$

$$C(T_c,R) = C_0 + C_1 R^{-\alpha/r\nu} \quad \text{for} \quad \alpha < 0, \tag{15}$$

$$C(T_c,R) \sim R^{-\alpha/r\nu} \quad \text{for} \quad \alpha > 0, \tag{16}$$

where C_1 is a constant. Fitting directly to Eqs. (13)–(16) can then give rise to the exponents.

C. Extended dynamic MCRG method

A direct realization of Eq. (6) is to use the method of extended dynamic MCRG [50–52], which is an extension of previous real-space MCRG methods [53]. The method has been detailed previously [50–52]. Here we give a brief description to collect relevant formulas. For a temperature sweep with a rate R, we perform a conventional block-spin transformation on the configuration at each time t (measured by MC steps per spin) corresponding to a temperature T by means of a majority rule with a length rescaling factor $b = 2$.

Ties are broken by a random selection from the two states. This RG transformation brings the system to a new state characterized by R', T', and t', which relate to their corresponding unblocked ones by Eq. (7) if scaling exists. In order to find these blocked variables, we resort to the peak of the correlation function G_{nn} of a system of size Lb and assume that it matches exactly after one blocking that of another smaller system of size L without blocked (so that the two systems whose G_{nn} is compared have the same size and thus size effects are reduced), viz.

$$G_{nn,Lb}(T_p',R') = G_{nn,L}(T_{ps},R_s), \tag{17}$$

where T_p represents the dynamic transition temperature corresponding to the temperature at the peak of G_{nn}, and the subscript s indicates quantities on the small lattice. In other words, we identify the primed variables with their counterparts on the small lattice. Accordingly,

$$r = \frac{\log(R_s/R)}{\log b},$$

$$\nu = \frac{\log b}{\log[(T_{ps} - T_c)/(T_p - T_c)]}. \tag{18}$$

Iterating this blocking procedure produces a series of exponents which should be invariant after a couple of blockings that iterate away the irrelevant variables if there is a fixed point controlling the scaling behavior because the correlation functions will then track each other.

Moreover, combining the first two equations of Eq. (7) at T_p, one finds an invariant constant

$$a \equiv \left(\frac{\tau_p}{R^{1/r\nu}}\right)' = \frac{\tau_p}{R^{1/r\nu}} \sim \left(\frac{\tau_p R^{-1}}{t_{eq}}\right)^{1/r\nu}, \tag{19}$$

under rescaling, where $t_{eq} \sim \tau_p^{-\upsilon z}$ is the correlation time at T_p, $\tau_p R^{-1}$ is the external time scale, and use has been made of Eq. (8) in deriving the last step, which reflects the similarity with finite-size scaling in which the ratio of the correlation length of a system of linear size L at T_c, $\xi_L(T_c)$ to L, $\xi_L(T_c)/L$ is scale invariant [54]. Therefore,

$$T_p = T_c + aR^{1/r\nu}, \tag{20}$$

which offers a method to estimate T_c [50,52] and a consistent check of the obtained exponents. Equation (20) is reasonable because at $R=0$ or equilibrium the correlation function ought to exhibit a peak at T_c. At a finite-time scale R^{-1}, there is an overshoot or hysteresis embodied in T_p due to the driving out of equilibrium.

We shall first determine T_c and then apply the extended dynamic MCRG method to determine ν, z, and r, on the basis of which, other exponents are estimated from the finite-time scaling.

III. NUMERICAL RESULTS

In order to study the influence of disorder from the random bonds we choose $r_0=2$, 4, 5, and 10. The pair of lattice sizes used is 128 and 64. Periodic boundary conditions are applied throughout. The sweep rate of the small lattice ranges from 3×10^{-5} to 1×10^{-2} and that of the large lattice from 3×10^{-5} to 3×10^{-4} for $r_0=2$, 4, and 5, while that for $r_0=10$ from 5×10^{-5} to 5×10^{-4} because of stronger fluctuations that demand more samples. For a given r_0 and R, we choose an initial temperature so far away from the transition temperature that it has been checked to have no effect on the results. Then, with one sample of a given realization of the disorder, we run a MC simulation from the initial temperature and a completely ordered state with all spins $S_i=1$. After one MC step consisting of a sequential sampling of all the spins in the lattice with the usual Metropolis algorithm [40], the temperature T is increased by the rate R. The system then evolves with time and transforms finally to a disordered state. The number of samples for average varies from 300 to 20 000 depending on lattice size and sweep rate used.

TABLE I. Estimated and fitted critical temperature and other fitted parameters with various r_0.

r_0	2	4	5	10
T_c'	6.701	10.914	12.990	23.272
T_c	6.720(9)	10.964(10)	13.057(7)	23.439(15)
$1/r\nu$	0.431(13)	0.409(11)	0.401(10)	0.386(10)
a	2.9(5)	3.3(3)	3.6(2)	5.6(2)

A. Critical temperature T_c

Fitting of T_p vs R to Eq. (20) yields the critical temperature. We use the data on the small lattice since more samples are available. No finite-size effects, however, have been found owing to the finite R^{-1} and ξ. Table I collects the fitting results for all r_0, where standard deviations from the fitting are shown in the parentheses. The obtained T_c shows almost a linear dependence on r_0 as can be seen from Fig. 1. Indeed, the fit gives $T_c(r_0=1)=4.67(5)$, which is close to $T_0=4.511\,528(6)$, the transition temperature of the pure system [55]. This linear dependence appears to be similar to the bond-diluted Ising model for not very large dilutions [11]. However, there is a significant difference here. Whereas in the bond-diluted case, there is a percolation dilution p_c at

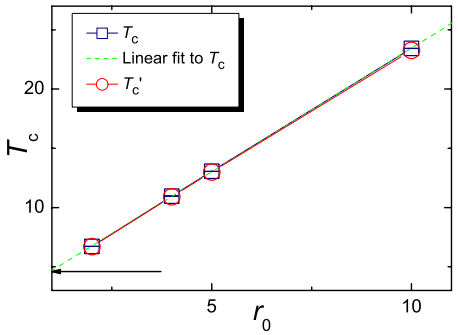

FIG. 1. (Color online) Dependence of the fitted (squares) and estimated (circles) critical temperatures on r_0. The errors arising from the fits are much smaller than the size of the symbols. The arrow marks the intercept at $r_0=0$ of the linear fit to T_c.

TABLE II. The exponents obtained by successive MCRG for various r_0.

		$m=1$				$m=2$				$m=3$				$m=4$			
r_0	R	r	ν	$1/r\nu$	z	r	ν	$1/r\nu$	z	r	ν	$1/r\nu$	z	r	ν	$1/r\nu$	z
2	3×10^{-5}	6.071	0.347	0.475	3.187	4.495	0.503	0.442	2.508	3.694	0.627	0.432	2.098	3.642	0.644	0.427	2.088
	5×10^{-5}	6.203	0.341	0.473	3.269	4.498	0.504	0.441	2.513	3.588	0.665	0.419	2.084	3.664	0.622	0.439	2.055
	7×10^{-5}	6.053	0.348	0.475	3.177	4.532	0.491	0.449	2.497	3.494	0.670	0.427	2.002	3.576	0.642	0.436	2.017
	1×10^{-4}	5.944	0.367	0.459	3.217	4.590	0.492	0.443	2.556	3.582	0.653	0.428	2.051	3.641	0.647	0.424	2.096
	3×10^{-4}	6.110	0.351	0.467	3.257	4.480	0.505	0.442	2.498	3.551	0.668	0.422	2.053	3.555	0.669	0.420	2.061
4	3×10^{-5}	6.474	0.379	0.408	3.833	4.329	0.547	0.422	2.501	3.521	0.690	0.412	2.072	3.364	0.674	0.412	2.119
	5×10^{-5}	6.385	0.387	0.405	3.799	4.325	0.556	0.416	2.526	3.640	0.669	0.411	2.144	3.604	0.710	0.403	2.085
	7×10^{-5}	6.221	0.389	0.413	3.651	4.305	0.558	0.416	2.512	3.518	0.697	0.409	2.083	3.633	0.678	0.406	2.159
	1×10^{-4}	6.103	0.398	0.412	3.588	4.287	0.562	0.415	2.509	3.582	0.654	0.427	2.052	3.563	0.683	0.411	2.098
	3×10^{-4}	6.805	0.398	0.413	3.571	4.240	0.564	0.418	2.467	3.641	0.667	0.412	2.141	3.552	0.703	0.401	2.129
5	3×10^{-5}	6.434	0.423	0.367	4.072	4.371	0.603	0.380	2.711	3.597	0.703	0.396	2.174	3.594	0.683	0.408	2.129
	5×10^{-5}	6.479	0.440	0.362	4.005	4.337	0.606	0.381	2.685	3.512	0.697	0.408	2.077	3.625	0.668	0.413	2.128
	7×10^{-5}	6.326	0.436	0.363	4.033	4.267	0.613	0.382	2.635	3.547	0.679	0.415	2.074	3.512	0.713	0.400	2.109
	1×10^{-4}	6.263	0.426	0.375	3.914	4.266	0.615	0.381	2.641	3.490	0.704	0.407	2.070	3.649	0.665	0.412	2.145
	3×10^{-4}	6.254	0.433	0.370	3.943	4.315	0.602	0.385	2.653	3.610	0.672	0.412	2.123	3.576	0.707	0.395	2.162
10	5×10^{-5}	6.581	0.427	0.356	4.237	4.379	0.669	0.341	2.886	3.541	0.746	0.379	2.201	3.403	0.795	0.370	2.145
	7×10^{-5}	6.599	0.420	0.361	4.220	4.336	0.658	0.351	2.816	3.561	0.745	0.377	2.218	3.472	0.770	0.374	2.173
	1×10^{-4}	6.407	0.415	0.376	3.996	4.348	0.616	0.374	2.724	3.430	0.774	0.376	2.139	3.440	0.784	0.371	2.165
	3×10^{-4}	5.877	0.441	0.386	3.607	4.243	0.615	0.383	2.618	3.543	0.762	0.371	2.229	3.495	0.739	0.387	2.143
	5×10^{-4}	5.735	0.443	0.394	3.478	4.212	0.605	0.392	2.560	3.457	0.756	0.383	2.135	3.486	0.779	0.368	2.203

which $T_c=0$, which deviates T_c from the linear dependence [11], here T_c is always finite even for $r_0\to\infty$ because $p=0.5$ is larger than the percolation threshold of $p_c\simeq0.248\,812\,6(5)$ of the 3D simple cubic lattice [56].

These fitted T_c can be well reproduced by an effective-interaction approximation [57]. In the single-bond approximation, the transition temperature T_c' for $p=0.5$ is given by [57]

$$\frac{1}{e^{2/T_c'-2/T_0}-1}+\frac{1}{e^{2r_0/T_c'-2/T_0}-1}+\frac{2p_c}{1-e^{-2/T_0}}=0. \quad (21)$$

The resultant T_c' are also listed in Table I and plotted in Fig. 1. It can be seen that they agree with our numerical results quite well although deviations increase slightly with disorder as fluctuations are stronger. For $r_0\to\infty$, $T_c'=2.04$, indeed different from 0. In fact, as $p=0.5$, $r_0=\infty$ is equivalent to $r_0=0$, and hence to the bond-diluted case with a dilution of the same p, which has a $T_c\approx2.07$ [11] in good agreement with ours. In addition, this T_c' is also not far away from the intercept $T_c(r_0=0)=2.588(46)$ of the linear fit in Fig. 1.

B. Exponents estimated by the dynamic MCRG

Applying the MCRG method with the obtained T_c then produces a series of exponents r, ν, $1/r\nu$, and z for each R of the large lattice as shown in Table II, where m is the number of iterations. One can see that they exhibit no systematic finite-time effects, i. e., no systematic dependence on R, and indeed tend to almost constant values after the second iteration, suggesting that irrelevant variables have been iterated away. However, results of the fifth iteration fluctuate a lot because of the small lattice size there. Accordingly, we average over those of the third and fourth iteration with the results shown in Table III, where in the parentheses are given standard deviations from the averages only. Errors arising from the RG have not been taken into account. One finds $1/r\nu$ indeed agrees well with that from fitting in Table I, showing its reliability and the consistency of our results. The dependence of r, ν, z, and $1/r\nu$ on r_0 are depicted in Fig. 2.

TABLE III. The critical exponents for various disorder amplitudes r_0.

r_0	r	ν	$1/r\nu$	z	β	α	γ	β/ν	γ/ν
2	3.60(6)	0.651(18)	0.427(7)	2.061(32)	0.374(6)	−0.035(16)	1.389(18)	0.575(18)	2.13(7)
4	3.57(5)	0.682(18)	0.410(7)	2.108(35)	0.349(6)	−0.046(17)	1.330(22)	0.512(16)	1.95(7)
5	3.57(5)	0.689(18)	0.407(7)	2.119(37)	0.343(6)	−0.052(17)	1.333(22)	0.498(16)	1.93(7)
10	3.48(5)	0.765(19)	0.376(6)	2.175(35)	0.354(6)	−0.130(29)	1.420(32)	0.463(17)	1.86(5)

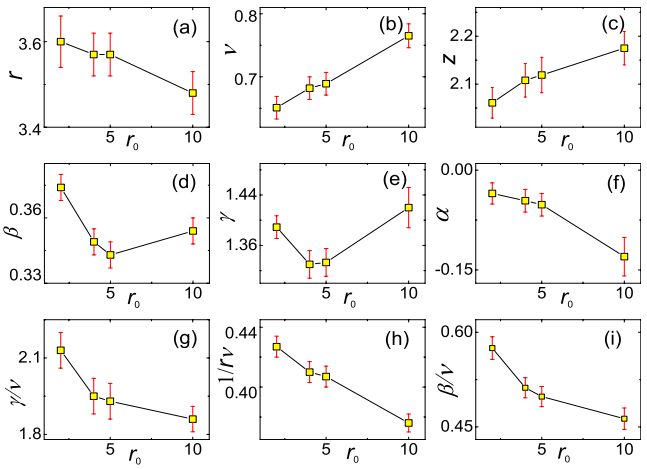

FIG. 2. (Color online) Variations in critical exponents with the disorder amplitudes r_0 for the 3D RBIM.

C. Exponents estimated by finite-time scaling

We have applied the finite-time scaling forms Eqs. (9), (10), and (12) to obtain β, γ, and α, respectively, in the 3D random-bond Potts model by searching the exponents that give optimal data collapses [47]. Here, we shall use directly Eqs. (13)–(15) instead. To this end, we find the values of M, χ, and C at $T=T_c$ for various R from 1×10^{-4} to 1×10^{-2} and every r_0 and fitting them according to Eqs. (13)–(15), respectively, as shown in Fig. 3. To check the resultant exponent ratios, we insert them along with T_c and $1/r\nu$ estimated above in Eqs. (9)–(11) and show the resulting scaling in Fig. 4. One sees that the curves collapse remarkably, confirming the exponents. We found that if we chose Eq. (16) to fit $C(T_c,R)$, we would obtain indeed a positive α, but then the data collapse according to Eq. (12) would be bad. This is just opposite to the case found in the 3D random-bond Potts model in which $\alpha>0$ [47].

From the exponent ratios, β, γ, and α can then be obtained. Their errors are estimated by error propagation. All results are shown also in Table III and Fig. 2.

IV. ANALYSIS AND DISCUSSION

As finite-size effects have been found to be important to the critical behavior in disordered systems, we first check the possible size effects of our results. We apply the dynamic MCRG method again to a smaller lattice pair of size 64 and 32 with $r_0=4$ as an instance. More samples (e.g., 3000 samples for $R=0.0001$) are used because of the strong fluctuations on small lattice sizes. The critical temperature and the hysteresis exponent obtained from fitting data on lattice sizes of $L=32$ are $T_c=10.969(10)$ and $1/r\nu=0.415(16)$, respectively, which agree well with previous results from $L=64$ in Table I. Estimates of the exponents for successive blockings are listed in Table IV. The averaged critical exponents over those from $m=3$ and $m=4$ in Table IV are compared with the results from the larger lattices in Table V, confirming that finite-size effects can be neglected for the two-lattice RG methods as expected.

Qualitatively, our ν increases with r_0, consistent with the results of the 3D bond-diluted Ising model [11] and also those found on the 3D four-state bond-diluted Potts models [58,60] and the 3D three-state random-bond Potts model [47]. Our γ shows a plateau near $r_0=4-5$ and increases when $r_0=10$, similar to that found in the high-temperature series expansion [8,59]. Our γ/ν and β/ν decrease with r_0, similar to those found in the 3D bond-diluted Ising model [11] but different from the 2D RBIM that appeared to show weak universality [44]. While the former is consistent with results found from the disordered Potts models [47,58], the latter is different from those on the Potts models in which it was found to be nonmonotonic [47,58,60]. In fact, this difference arises from the distinct variation in β with r_0. Whereas β there increases with r_0 [47] in agreement with results on the 3D site-diluted Ising model [11,21,61], here it shows a nonmonotonic variation, which agrees with that found in [62] by Heuer. Yet, the same author also found another variation trend of β in [15]. In spite of these differences that probably arise from crossover, we shall find later on that the asymptotic behavior appear right. In addition, in agreement with other studies [36,47,63], the increase in z with r_0 indicates reasonably slower critical relaxation, which implies in turn more severe hysteresis and hence a decreasing of $1/r\nu$. Also, our ν satisfies the bound $\nu\geq2/d$ [64] except that at $r_0=2$ which lies at the verge and $\alpha<0$ in the whole range of disorder strength in sharp contrast to the 3D random-bond Potts model [47].

In the extended MCRG method, we just recorded the resultant exponents in each blocking without monitoring the behavior of operators other than τ and R. However, as can be

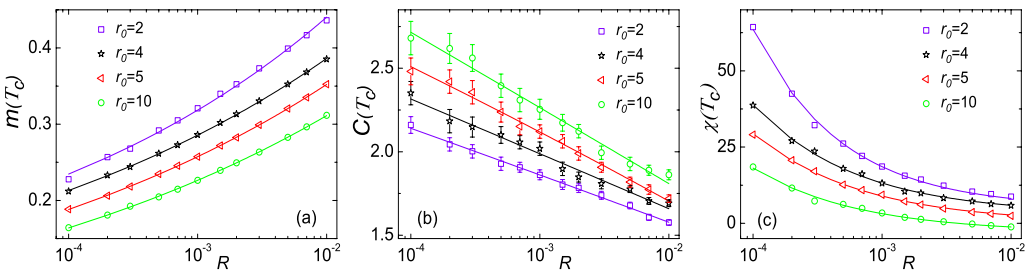

FIG. 3. (Color online) Dependence on R of (a) the order parameter M, (b) the specific heat C, and (c) the susceptibility χ at T_c. Lines are fits according to Eqs. (13)–(15). For clarity, the curves have been shifted vertically by 0.05, 0.03, 0, −0.01 in (a), −0.1, 0, 0.1, 0.3 in (b), and 5, 3, 0, −3 in (c) for $r_0=2$, 4, 5, and 10, respectively. Note that the error bars in (b) represent only the width of the C curves. The widths of the M and χ curves are tiny and thus are not shown.

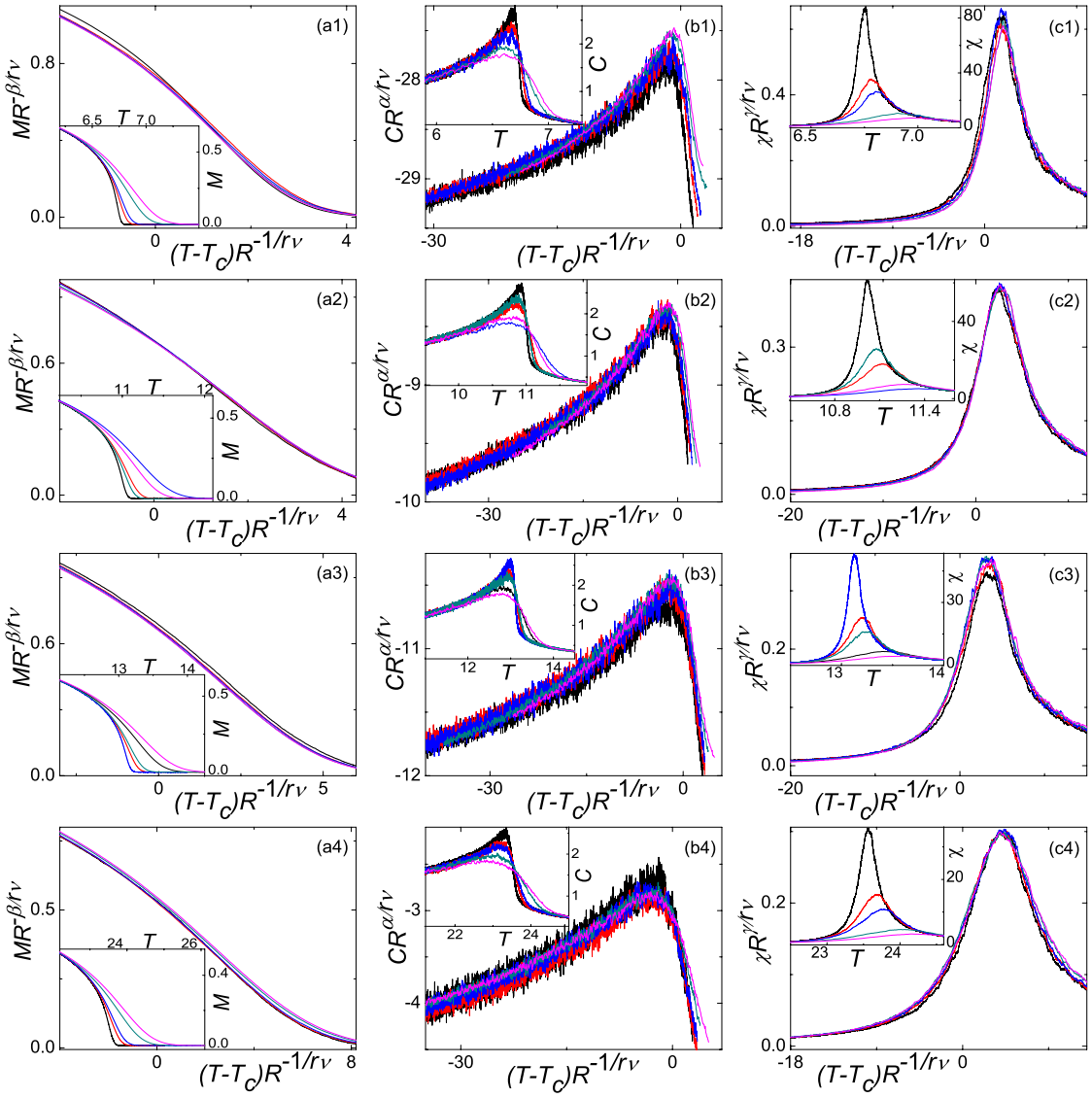

FIG. 4. (Color online) Finite-time scaling forms of the order parameter M, the specific heat C, and the susceptibility χ for r_0=2 (a1, b1, c1), 4 (a2, b2, c2), 5 (a3, b3, c3), and 10 (a4, b4, c4), respectively. Insets show the original curves. All curves are from the small lattice. The sweep rates are 0.0001, 0.0005, 0.001, 0.005, and 0.01 from left to right.

seen from Table II, the exponents obtained level off within statistical fluctuations in the third and fourth blockings. This indicates that all those irrelevant couplings should have been iterated away to those numbers of iterations. More importantly, as pointed out, the resultant $1/r\nu$ agrees well with that obtained directly from fitting the peak temperatures T_p. We have checked that if we chose a T_c with an appreciable deviation and inserted it into the MCRG method, the resultant $1/r\nu$ would not agree with that fitted from that T_c and would exhibit clear finite-time effects or would not level off. Ac-

TABLE IV. Exponents obtained from dynamic MCRG for the disorder amplitude r_0=4 and a lattice pair of 64 and 32.

	$m=1$				$m=2$				$m=3$				$m=4$			
R	r	ν	$1/r\nu$	z	r	ν	$1/r\nu$	z	r	ν	$1/r\nu$	z	r	ν	$1/r\nu$	z
3×10^{-5}	6.674	0.379	0.395	4.035	4.364	0.568	0.404	2.603	3.620	0.691	0.400	2.173	3.440	0.705	0.413	2.021
5×10^{-5}	6.486	0.387	0.398	3.902	4.355	0.557	0.413	2.558	3.440	0.669	0.434	1.946	3.534	0.691	0.410	2.087
7×10^{-5}	6.221	0.389	0.413	3.652	4.205	0.558	0.426	2.414	3.497	0.708	0.404	2.085	3.571	0.689	0.406	2.120
1×10^{-4}	6.103	0.398	0.412	3.590	4.256	0.573	0.410	2.510	3.613	0.695	0.399	2.174	3.461	0.653	0.442	1.930
3×10^{-4}	5.823	0.408	0.421	3.372	4.240	0.565	0.418	2.468	3.574	0.657	0.426	2.051	3.633	0.683	0.403	2.170

TABLE V. Exponents obtained from different lattice sizes for the 3D RBIM with $r_0=4$.

Lattice size	r	ν	$1/r\nu$	z
128–64	3.57(5)	0.682(17)	0.410(7)	2.108(35)
64–32	3.53(7)	0.684(15)	0.414(15)	2.08(9)

cordingly, the consistency of T_c and $1/r\nu$ between the two methods should provide a strong evidence for their reliability.

Figures 3 and 4 show that Eqs. (9)–(11) describe our numerical results quite well. This implies that corrections to scaling that have been found to be important [10,16] are not significant here. Assume that the leading irrelevant variable is Y and its corresponding exponent $\omega>0$, Eq. (6) is modified to

$$M(T,R,Y) = b^{-\beta/\nu} M(\tau b^{1/\nu}, Rb^{r}, Yb^{-\omega}). \tag{22}$$

Accordingly, Eq. (9) becomes

$$M(T,R,Y) = R^{\beta/r\nu} f_5(\tau R^{-1/r\nu}, YR^{\omega/r}), \tag{23}$$

where f_5 is anther scaling function. So, even at $\tau=0$,

$$M(T_c,R,Y) = R^{\beta/r\nu} f_6(YR^{\omega/r}). \tag{24}$$

It is the scaling function f_6 that induces the leading corrections to scaling [65]. Exactly at the critical point, $R=0$ and the corrections disappear, while near it, one can expand $f_6(x)$ at $x=0$ as a series of $YR^{\omega/r}$ to find ω/r. If these terms were important, $M(T_c,R)$ would not be a pure power law as shown in Fig. 3 and all the curves shown in the inset in Fig. 4 within a remarkable two orders of magnitude could not collapse. So, why do these corrections appear absent?

A possible reason is the following. The corrections are $YL^{-\omega}$ in finite-size scaling and $Yt^{-\omega/z}$ in short-time critical dynamics [19]. We note that generally, the corrections have bigger magnitudes in finite-time scaling. Because, for $|Y|R^{\omega/r} \leq |Y|L^{-\omega}$, R must smaller than L^{-r}, which, for $L=100$ and $r=4$, is 10^{-8}, a figure which is out of our present reach. The reason that the corrections are not significant lies possibly in the smallness of ω/r in comparison to ω and ω/z because r is large from Eq. (8), usually about 4. As result, $YR^{\omega/r}$ varies little and can be taken as a constant and hence ignored within a practical range of R in comparison to the other two cases. For example, for the corrections to be half, L needs only to increase to $2^{1/\omega}\sim 10$ times that are usually available but R must decrease to r powers of that number that is about 10^4 for $\omega=0.3$ [7,16] and $r=4$. Although the first arguments in Eq. (23) and its counterparts also change identical amounts by these same ranges if τ does not change, the latter in fact varies with scales and thus they cannot be simply compared. These then indicate that the importance of the corrections to scaling increases from finite-time scaling to short-time critical dynamics to finite-size scaling. For the present case, $\omega/r\sim 0.1$ is small. As a result, to precisely estimate it and other critical exponents, one may need a wide range of R. However, one sees that our results acquire comparable precisions with other usual methods even though we have not taken corrections into account.

TABLE VI. The values of $\alpha+d\nu$, $\alpha+2\beta+\gamma$, and $2\beta/\nu+\gamma/\nu$ of the 3D random-bond Ising model for various disorder amplitudes.

r_0	Exact value	2	4	5	10
$\alpha+d\nu$	2	1.92(6)	2.00(6)	2.01(6)	2.17(6)
$\alpha+2\beta+\gamma$	2	2.10(3)	1.98(3)	1.97(3)	2.00(5)
$2\beta/\nu+\gamma/\nu$	3	3.28(10)	2.97(9)	2.93(8)	2.79(8)

In order to reveal the nature of the exponents, we now test the hyperscaling law $\alpha+d\nu=2$, the Rushbrooke scaling law $\alpha+2\beta+\gamma=2$, and their combined scaling law $2\beta/\nu+\gamma/\nu=d$ [2] in Table VI. One finds that all the three laws are satisfied for $r_0=4$ and 5. As finite-size effects and corrections to scaling have been shown to be absent or unimportant, this leads us to believe that the exponents within $r_0=4$ and 5 are asymptotic ones. Moreover, there exists another evidence for the asymptotic nature of the exponents in the middle region. Taking into account the error bars, one notices that all exponents shown in Fig. 2 exhibit plateaux at least for $4\lesssim r_0 \lesssim 5$ similar to the case of series expansions [8,59]. In fact, similar reasoning of whether a scaling law is satisfied [7,58] or there is a plateau in the variation with disorder strength [8,59] has been invoked to identify asymptotic critical exponents. Therefore, we conclude that those exponents at least within $4\leq r_0\leq 5$ are the asymptotic critical ones controlled by the random fixed point. Averaging over them, we obtain our final estimates of the critical exponents for the fixed point as

$$\nu = 0.686(25), \quad \beta = 0.346(8), \quad \alpha = -0.049(24),$$

$$\gamma = 1.332(31), \quad z = 2.114(51), \quad r = 3.57(7),$$

$$1/r\nu = 0.409(10), \quad \beta/\nu = 0.505(23), \quad \gamma/\nu = 1.94(10). \tag{25}$$

One sees that our ν and β agree well with previous results [6,7,10–12,19,20,22]. So does γ that appears not to support that of the nonperturbative RG [20] and series expansions [59] albeit not far away when taking the error into account. Our α also support the RG [7] and MC results [7,10–12,16,18,19] but not the experimental one [6]. Our z closes to recent RG [26–32], MC [13,19], as well as experimental results [33,34], but not support the larger values of $z\approx 2.6$ [37,38] and $z\approx 2.35$ [14,39]. Reversely, the agreement of our results with others implies that the three scaling laws tested are indeed satisfied in the 3D disordered Ising model.

For the exponents at the two ends, one sees from Table VI that some scaling laws are satisfied or nearly satisfied but not all are satisfied. In particular, the third law is violated in both cases. This is at odd with the random-bond Potts model in which exponents at the two ends all satisfy the third law but not the other two laws [47]. Also, effective exponents of the bond-diluted Ising model were also found to satisfied the

third law [11]. This may stem from the different proximity to the fixed point [28]. As corrections to scaling are not important especially for $r_0=2$ as seen in Fig. 3, the exponents that dissatisfied the scaling laws cannot be asymptotic except unlikely the scaling laws are themselves violated. Accordingly, the most likely scenario is that the exponents in $r_0 \lesssim 4$ and $r_0 \gtrsim 5$ are, similar to the Potts model [47], crossover ones that reflect the crossover from the pure fixed point to the random fixed point and the latter to the percolation fixed point in the system, respectively. In addition, although whether or not crossover exponents should satisfy scaling laws is still an open problem [66], our results seem to indicate that at least not all of them are satisfied in these two cases. In other words, validating of a single or even two scaling laws may not be invoked as an indication of the asymptotic nature.

Now we turn to the question of the possible existence of two universality classes. It was found by a finite-size scaling method without considering corrections to scaling that for a spin concentration $p=0.6$, $\nu=0.725(6)$, $\gamma=1.446(4)$, $\alpha=-0.093(7)$, and $\beta=0.349(4)$, which were different from the lower disorder ones and thus were suggested to belong to a new class [21]. Similar results were also obtained when considering corrections [18]. One finds from Table III that our corresponding exponents for $r_0=10$ are quite close to those numbers. This seems to indicate that their results may just also be crossover exponents that reflect the crossover to the percolation fixed point. In fact, using their exponents listed, one finds $\alpha+d\nu=2.082(19)$, $\alpha+2\beta+\gamma=2.051(11)$, and $2\beta/\nu+\gamma/\nu=2.957(27)$. Accordingly, one sees that the first two laws are broken by 4–5 times of their respective standard errors and the third one by about two times. In addition, their exponents vary with p [21]. So do those in [18]. Consequently, these exponents [18,21] may be more probably crossover than a new class.

In order to distinguish possible different universality classes among the site-diluted, the bond-diluted, the $\pm J$, and the RBIM, we list in Table VII the critical exponents of the four kinds of disordered Ising model, along with the six-loop RG results of random Ising model. One sees clearly that the exponents all agree quite well, confirming the universality of the fixed point with respect to the forms of disorder.

TABLE VII. The critical exponents for the site-diluted Ising model (SDIM), the bond-diluted Ising model (BDIM), the $\pm J$ Ising model ($\pm J$IM), and the present random-bond Ising model (RBIM). The six-loop RG results of the random Ising model (RIM) are also listed for comparison.

Model	ν	β	γ	α
RIM (RG)[a]	0.678(10)	0.349(5)	1.330(17)	−0.034(30)
SDIM[b]	0.681(2)	0.354(1)	1.341(4)	−0.049(6)
BDIM[c]	0.68(2)	0.35(1)	1.34(1)	−0.04(6)
$\pm J$IM [b]	0.682(3)	0.354(8)	1.339(7)	−0.046(9)
RBIM (here)	0.686(25)	0.346(8)	1.332(31)	−0.049(24)

[a]Reference [7].
[b]Reference [16].
[c]Reference [11].

V. CONCLUSION

We have investigated the critical behavior of 3D RBIM for $r_0=2$, 4, 5, and 10 by the finite-time scaling combining with MCRG method in the presence of the linearly varying temperature. The method enables us to estimate a lot of critical exponents independently as well as the critical temperatures. Our results listed in Eq. (25) show that the static exponents agree well with most existing results and the dynamic critical exponent of $z=2.114(51)$ support a lower value found by RG analyses, experiments, and some MC simulations. They also verify both the hyperscaling and the Rushbrooke scaling laws and their combined scaling law, which in turn validate their asymptotic nature. In addition, they corroborate the universality of the site-diluted, the bond-diluted, the $\pm J$, and the RBIM. The exponents at $r_0=2$ and $r_0=10$ are argued to be crossover exponents that reflect crossover from the random fixed point to the pure and the percolation fixed point and that do not satisfy all scaling laws. So, validating of a single or even two scaling laws may not be invoked as an indication of the asymptotic nature of the obtained exponents. In addition, the crossover exponents at $r_0=10$ appear to close to those that were proposed to constitute a distinct universality class. This indicates that they are probably also crossover only. Our results also demonstrate that the finite-time scaling method can directly probe both static and dynamic critical behavior without taking corrections to scaling into account with reasonable precisions due to the small correction exponent for the method.

ACKNOWLEDGMENT

This work was supported by the NNSF of PRC (Grant No. 10625420).

[1] A. B. Harris, J. Phys. C **7**, 1671 (1974).
[2] J. Cardy, *Scaling and Renormalization in Statistical Physics* (Cambridge University Press, Cambridge, 1996).
[3] For reviews, see, V. S. Dotsenko and V. S. Dotsenko, Adv. Phys. **32**, 129 (1983); B. N. Shalaev, Phys. Rep. **237**, 129 (1994).
[4] R. Guida and J. Zinn-Justin, J. Phys. A **31**, 8103 (1998).
[5] For a review, see R. Folk, Yu. Holovatch, and T. Yavors'kii, Phys. Usp. **46**, 169 (2003).
[6] For a review, see D. P. Belanger, Braz. J. Phys. **30**, 682 (2000).
[7] A. Pelissetto and E. Vicari, Phys. Rev. B **62**, 6393 (2000).
[8] M. Hellmund and W. Janke, Phys. Rev. B **74**, 144201 (2006).
[9] S. Wiseman and E. Domany, Phys. Rev. Lett. **81**, 22 (1998); Phys. Rev. E **58**, 2938 (1998); A. Aharony, A. B. Harris, and S. Wiseman, Phys. Rev. Lett. **81**, 252 (1998).

[10] H. G. Ballesteros, L. A. Fernández, V. Martín-Mayor, A. Muñoz Sudupe, G. Parisi, and J. J. Ruiz-Lorenzo, Phys. Rev. B **58**, 2740 (1998).
[11] P. E. Berche, C. Chatelain, B. Berche, and W. Janke, Eur. Phys. J. B **38**, 463 (2004); Comput. Phys. Commun. **147**, 427 (2002).
[12] P. Calabrese, V. Martín-Mayor, A. Pelissetto, and E. Vicari, Phys. Rev. E **68**, 036136 (2003).
[13] D. Ivaneyko, J. Ilnytskyi, B. Berche, and Yu. Holovatch, Physica A **370**, 163 (2006); Condens. Matter Phys. **8**, 149 (2005).
[14] P. Calabrese, A. Pelissetto, and E. Vicari, Phys. Rev. E **77**, 021126 (2008).
[15] H. O. Heuer, J. Phys. A **26**, L333 (1993).
[16] M. Hasenbusch, F. P. Toldin, A. Pelissetto, and E. Vicari, J. Stat. Mech.: Theory Exp. (2007) P02016.
[17] K. Hukushima, J. Phys. Soc. Jpn. **69**, 631 (2000).
[18] V. V. Prudnikov, P. Prudnikov, A. Vakilov, and A. Krinitsyn, Sov. Phys. JETP **105**, 371 (2007).
[19] V. V. Prudnikov, P. V. Prudnikov, A. S. Krinitsyn, A. N. Vakilov, E. A. Pospelov, and M. V. Rychkov, Phys. Rev. E **81**, 011130 (2010).
[20] M. Tissier, D. Mouhanna, J. Vidal, and B. Delamotte, Phys. Rev. B **65**, 140402(R) (2002).
[21] A. K. Murtazaev, I. K. Kamilov, and A. B. Babaev, Sov. Phys. JETP **99**, 1201 (2004); A. K. Murtazaev and A. B. Babaev, J. Magn. Magn. Mater. **321**, 2630 (2009).
[22] D. V. Pakhnin and A. I. Sokolov, JETP Lett. **71**, 412 (2000); Phys. Rev. B **61**, 15130 (2000).
[23] G. Grinstein, Phys. Rev. Lett. **37**, 944 (1976); D. S. Fisher, *ibid.* **56**, 416 (1986).
[24] A. J. Bray, T. McCarthy, M. A. Moore, J. D. Reger, and A. P. Young, Phys. Rev. B **36**, 2212 (1987); A. J. McKane, *ibid.* **49**, 12003 (1994); G. Álvarez, V. Martín-Mayor, and J. J. Ruiz-Lorenzo, J. Phys. A **33**, 841 (2000).
[25] G. Grinstein, S.-k. Ma, and G. F. Mazenko, Phys. Rev. B **15**, 258 (1977).
[26] M. S. Li and F. T. Tela, Sov. Phys. Solid State **26**, 786 (1984).
[27] V. V. Prudnikov and A. N. Vakilov, Sov. Phys. JETP **74**, 990 (1992) [Pis'ma Zh. Eksp. Teor. Fiz. **101**, 1853 (1992)].
[28] H. K. Janssen, K. Oerding, and E. Sengespeick, J. Phys. A **28**, 6073 (1995).
[29] K. Oerding, J. Phys. A **28**, L639 (1995).
[30] V. V. Prudnikov, S. V. Belim, E. V. Osintsev, and A. A. Fedorenko, Phys. Solid State **40**, 1383 (1998).
[31] V. Blavats'ka, M. Dudka, R. Folk, and Yu. Holovatch, Phys. Rev. B **72**, 064417 (2005).
[32] A. Krinitsyn, V. Prudnikov, and P. Prudnikov, Theor. Math. Phys. **147**, 561 (2006).
[33] N. Rosov, C. Hohenemser, and M. Eibschutz, Phys. Rev. B **46**, 3452 (1992).
[34] Z. Slanič, D. P. Belanger, and J. A. Fernandez-Baca, Phys. Rev. Lett. **82**, 426 (1999).
[35] V. V. Prudnikov and A. N. Vakilov, JETP Lett. **55**, 741 (1992) [Pis'ma Zh. Eksp. Teor. Fiz. **55**, 709 (1992)].
[36] H. O. Heuer, J. Phys. A **26**, L341 (1993).
[37] G. Parisi, F. Ricci-Tersenghi, and J. J. Ruiz-Lorenzo, Phys. Rev. E **60**, 5198 (1999).
[38] G. Schehr and R. Paul, Phys. Rev. E **72**, 016105 (2005).
[39] M. Hasenbusch, A. Pelissetto, and E. Vicari, J. Stat. Mech.: Theory Exp. (2007) P11009.
[40] N. Metropolis, A. W. Rosenbluth, M. N. Rosenbluth, A. M. Teller, and E. Teller, J. Chem. Phys. **21**, 1087 (1953).
[41] R. H. Swendsen and J.-S. Wang, Phys. Rev. Lett. **58**, 86 (1987).
[42] U. Wolff, Phys. Rev. Lett. **62**, 361 (1989).
[43] M. Hennecke and U. Heyken, J. Stat. Phys. **72**, 829 (1993).
[44] J.-K. Kim, Phys. Rev. B **61**, 1246 (2000).
[45] S. Gong, F. Zhong, X. Huang, and S. Fan, New J. Phys. **12**, 043036 (2010); X. Huang, S. Gong, F. Zhong, and S. Fan, Phys. Rev. E **81**, 041139 (2010).
[46] S. Fan and F. Zhong, Phys. Rev. E **79**, 011122 (2009).
[47] W. Xiong, F. Zhong, and S. Fan (unpublished).
[48] S. Shinomoto and Y. Kabashima, J. Phys. A **24**, L141 (1991).
[49] K. Hukushima and K. Nemeto, J. Phys. Soc. Jpn. **64**, 1863 (1995); H. Shima and T. Nakayama, *ibid.* **67**, 2189 (1998).
[50] F. Zhong, Phys. Rev. B **66**, 060401(R) (2002); F. Zhong and Z. Xu, *ibid.* **71**, 132402 (2005).
[51] F. Zhong, Phys. Rev. E **73**, 047102 (2006).
[52] S. Fan and F. Zhong, Phys. Rev. E **76**, 041141 (2007).
[53] S. K. Ma, Phys. Rev. Lett. **37**, 461 (1976); R. H. Swendsen, *ibid.* **42**, 859 (1979); J. Tobochnik, S. Sarker, and R. Cordery, *ibid.* **46**, 1417 (1981); S. L. Katz, J. D. Gunton, and C. P. Liu, Phys. Rev. B **25**, 6008 (1982).
[54] D. J. Amit and V. Martin-Mayor, *Field Theory, the Renormalization Group, and Critical Phenomena*, 3rd ed. (World Scientific Press, Singapore, 2005).
[55] A. L. Talapov and H. W. J. Blote, J. Phys. A **29**, 5727 (1996).
[56] C. D. Lorenz and R. M. Ziff, Phys. Rev. E **57**, 230 (1998).
[57] L. Turban, J. Phys. C **13**, L13 (1980); Phys. Lett. A **75**, 307 (1980).
[58] C. Chatelain, B. Berche, and W. Janke, and P. E. Berche, Nucl. Phys. B **719**, 275 (2005).
[59] M. Hellmund and W. Janke, Phys. Rev. E **67**, 026118 (2003); Condens. Matter Phys. **8**, 59 (2005).
[60] J. Q. Yin, B. Zheng, and S. Trimper, Phys. Rev. E **72**, 036122 (2005).
[61] J. Marro, A. Labarta, and J. Tejada, Phys. Rev. B **34**, 347 (1986); D. Chowdhury and D. Staufer, J. Stat. Phys. **44**, 203 (1986).
[62] H. O. Heuer, Europhys. Lett. **12**, 551 (1990); Phys. Rev. B **42**, 6476 (1990).
[63] J. Q. Yin, B. Zheng, V. V. Prudnikov, and S. Trimper, Eur. Phys. J. B **49**, 195 (2006).
[64] J. T. Chayes, L. Chayes, D. S. Fisher, and T. Spencer, Phys. Rev. Lett. **57**, 2999 (1986).
[65] F. W. Wegner, Phys. Rev. B **5**, 4529 (1972).
[66] D. O'Connor and C. R. Stephens, Phys. Rep. **363**, 425 (2002).